

Mediating anion-cation interactions to improve aqueous flow battery electrolytes

David Reber^{1*}, Jonathan R. Thurston², Maximilian Becker^{3,4}, Gregory F. Pach⁵, Marc E. Wagoner²,
Brian H. Robb⁶, Scott E. Waters², Michael P. Marshak^{1,2*}

- 1) Renewable and Sustainable Energy Institute, University of Colorado Boulder, Boulder, CO 80303, USA
- 2) Department of Chemistry, University of Colorado Boulder, Boulder, CO 80309, USA
- 3) Empa, Swiss Federal Laboratories for Materials Science and Technology, 8600 Dübendorf, Switzerland
- 4) ETH Zürich, Department of Materials, 8093 Zurich, Switzerland
- 5) Chemistry and Nanoscience Center, National Renewable Energy Laboratory, Golden, CO, 80401, USA
- 6) Department of Chemical and Biological Engineering, University of Colorado Boulder, Boulder, CO 80303, USA

*E-mail: david.reber@colorado.edu, michael.marshak@colorado.edu

Supporting Information

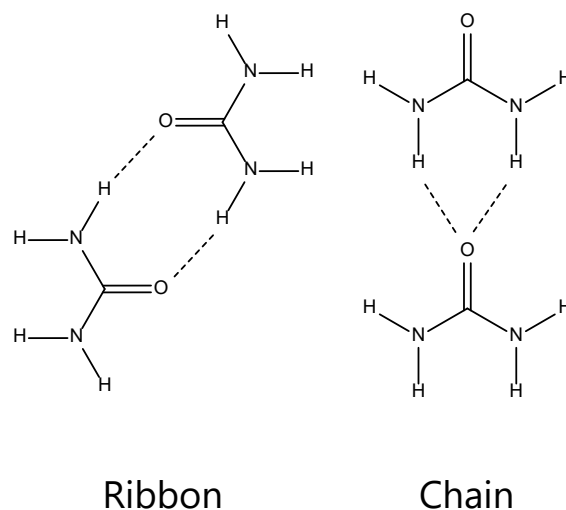


Fig. S1: Structure of a urea ribbon and a chain dimer, based on reference [1].

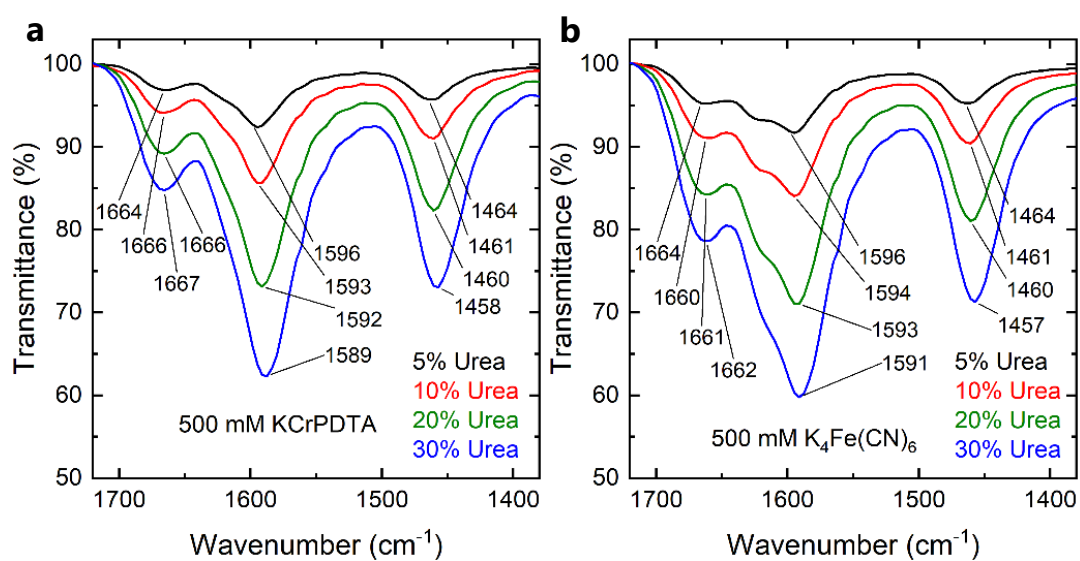


Fig. S2: IR spectra of urea solutions with **a**, 500 mM KCrPDТА or **b**, K₄Fe(CN)₆. The spectra of 500 mM respective salt in pure water were subtracted to obtain the urea signatures.

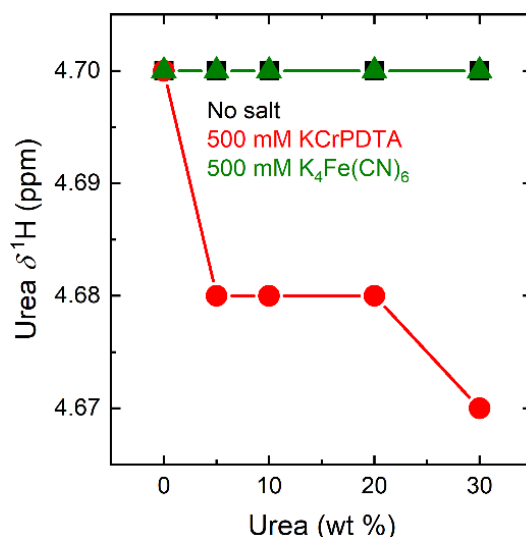


Fig. S3: NMR chemical shifts $\delta^1\text{H}$ of water in water, 500 mM KCrPDTA, or $\text{K}_4\text{Fe}(\text{CN})_6$ solutions, respectively.

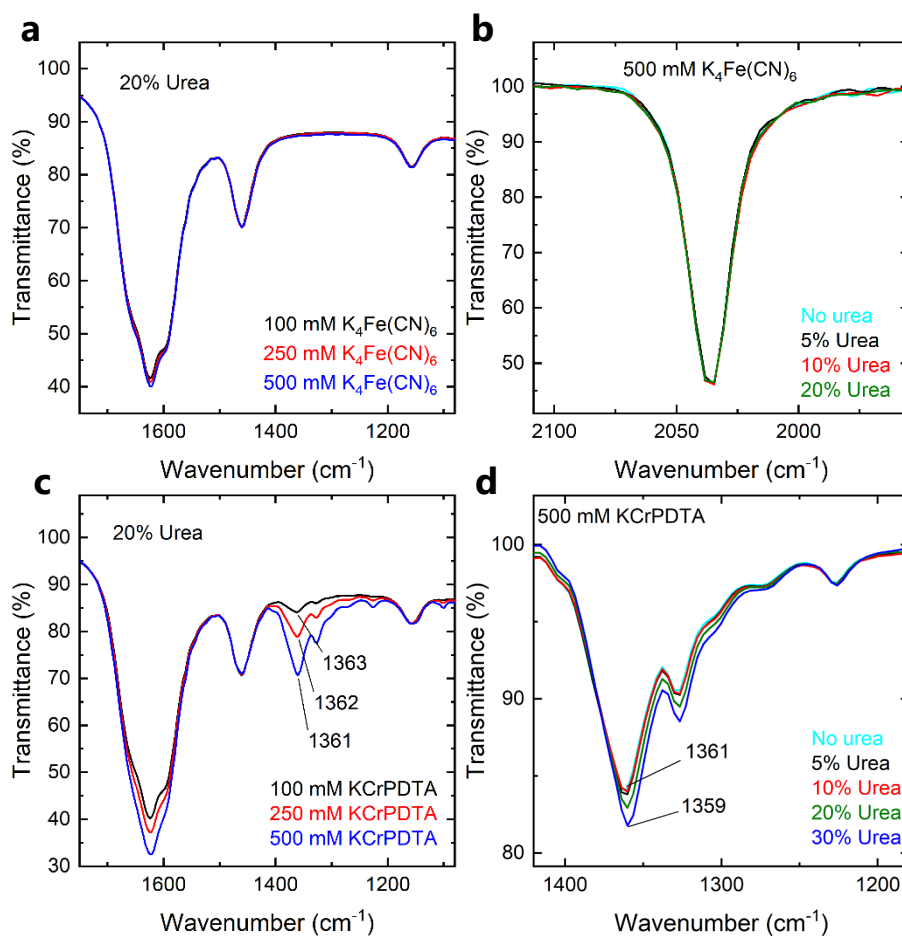


Fig. S4: Raw IR spectra of **a**, 100 mM, 250 mM and 500 mM $\text{K}_4\text{Fe}(\text{CN})_6$ solutions with 20% urea, **b**, 500 mM $\text{K}_4\text{Fe}(\text{CN})_6$ at different urea concentrations, **c**, 100 mM, 250 mM and 500 mM KCrPDTA solutions with 20% urea, and **d**, 500 mM KCrPDTA at different urea concentrations. For samples in a and c no references were subtracted.

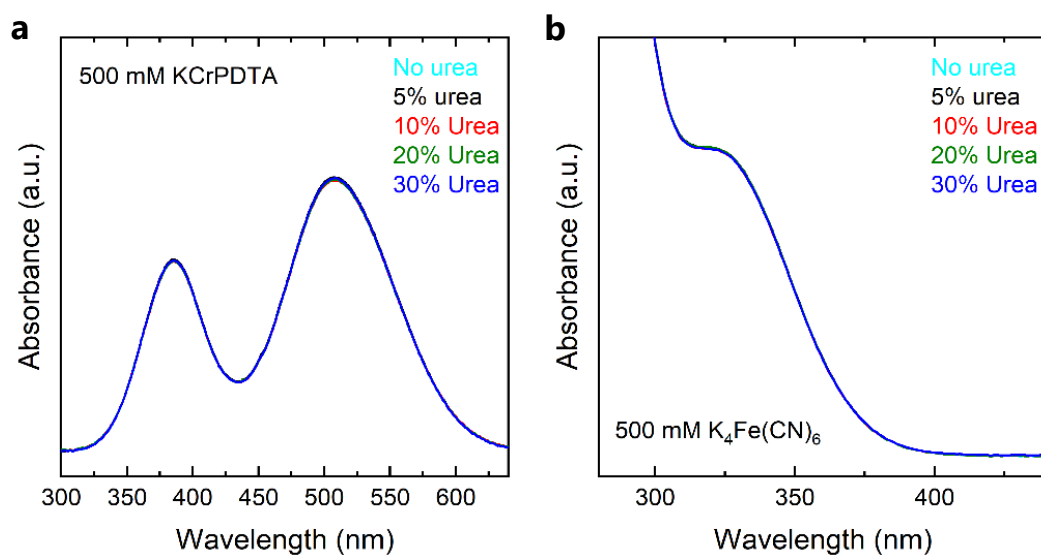


Fig. S5: UV-vis spectra of urea solutions with **a**, 500 mM KCrPDTA (diluted 250x) or **b**, 500 mM $K_4Fe(CN)_6$ (diluted 500x).

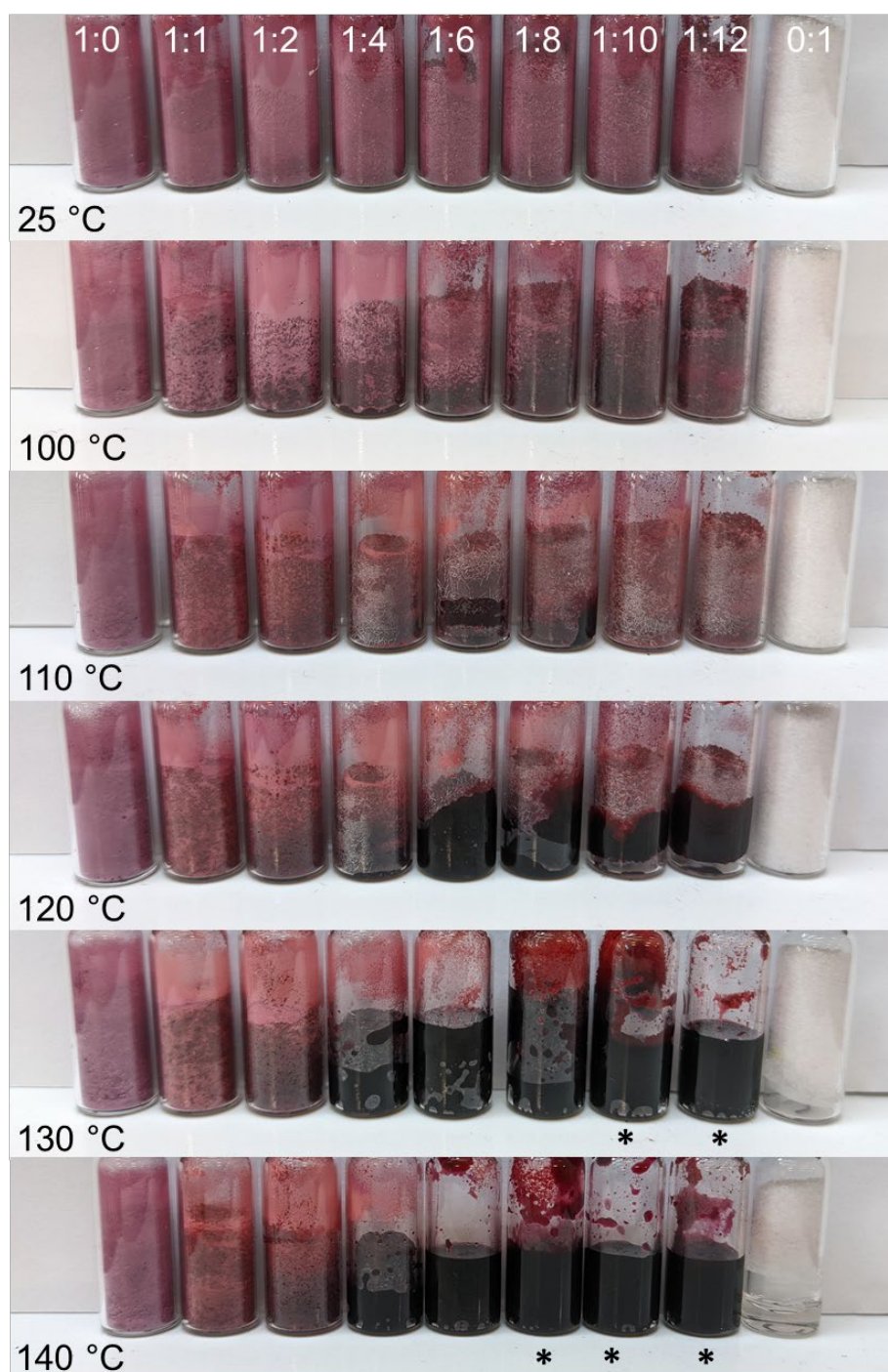


Fig. S6: Qualitative assessment of melting points of dry KCrPDTA:urea mixtures with increasing molar fractions of urea from left to right. Samples marked with a * are completely liquid. For reference, urea (melting point 133 °C) starts melting at a hotplate temperature of 130 – 140 °C.

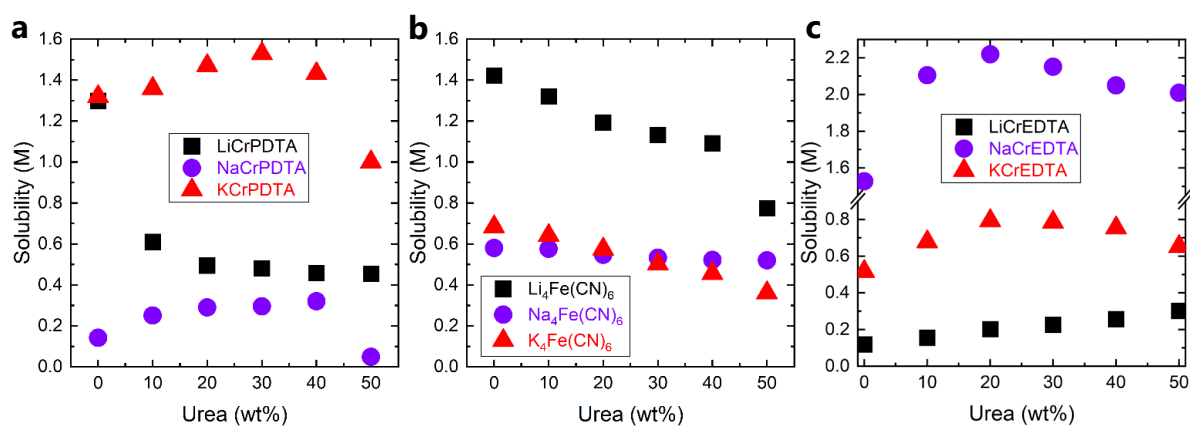


Fig. S7: Maximum solubility at room temperature of **a**, LiCrPDTA, NaCrPDTA, and KCrPDTA, **b**, $\text{Li}_4\text{Fe}(\text{CN})_6$, $\text{Na}_4\text{Fe}(\text{CN})_6$, and $\text{K}_4\text{Fe}(\text{CN})_6$, and **c**, LiCrEDTA, NaCrEDTA, and KCrEDTA in aqueous urea solutions.

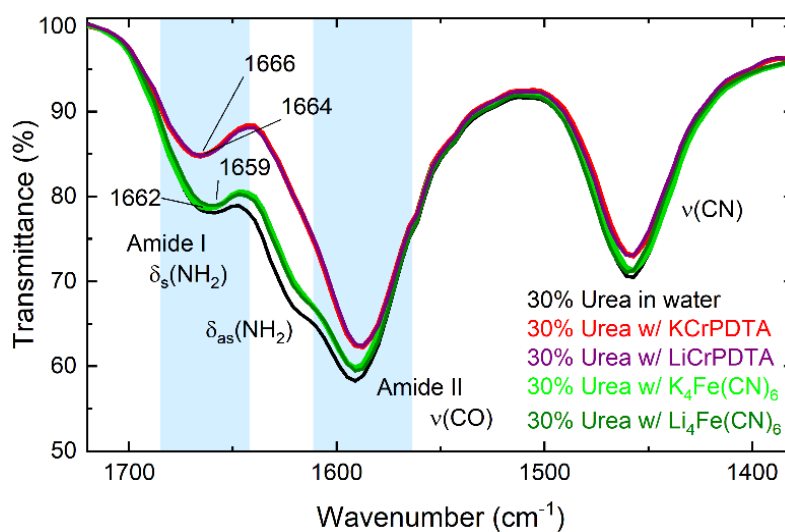


Fig. S8: **a**, IR spectra of 30% urea solutions with either 500 mM KCrPDTA or $\text{K}_4\text{Fe}(\text{CN})_6$ or lithium analogues, respectively. The spectra of 500 mM respective salt in pure water were subtracted to obtain the urea signatures. Urea bands in 30% urea in water are shown for comparison.

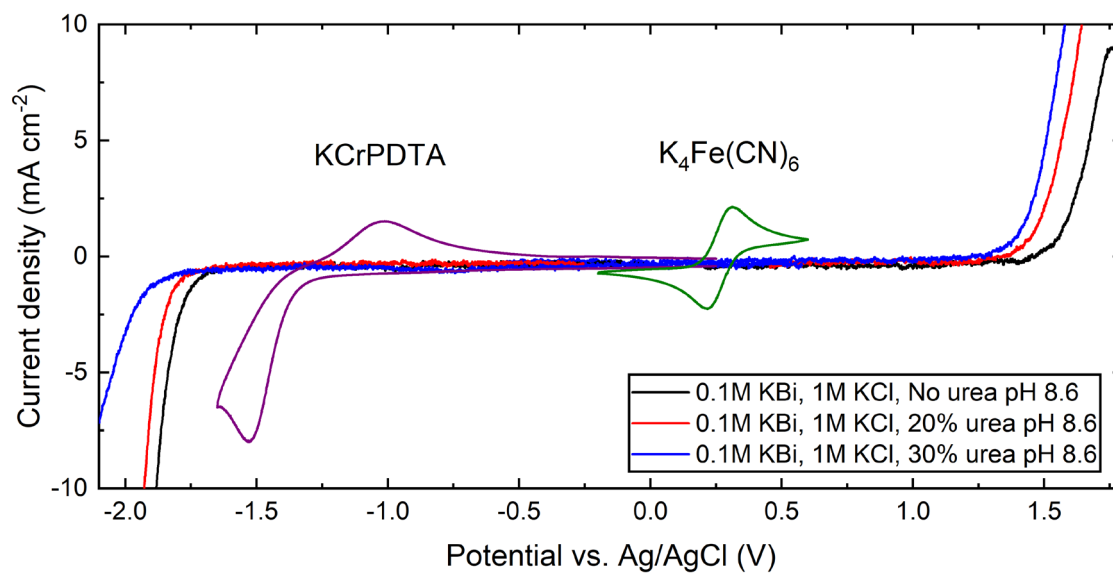


Fig. S9: Linear sweep voltammograms of buffered 1 M KCl solutions containing 0%, 20%, or 30% urea at pH 8.6 on glassy carbon electrodes. The scan rate was set to 10 mV s⁻¹. Cyclic voltammograms of KCrPDTA and K₄Fe(CN)₆ solutions are also shown. The current densities for the active material measurements were scaled for easier comparison.

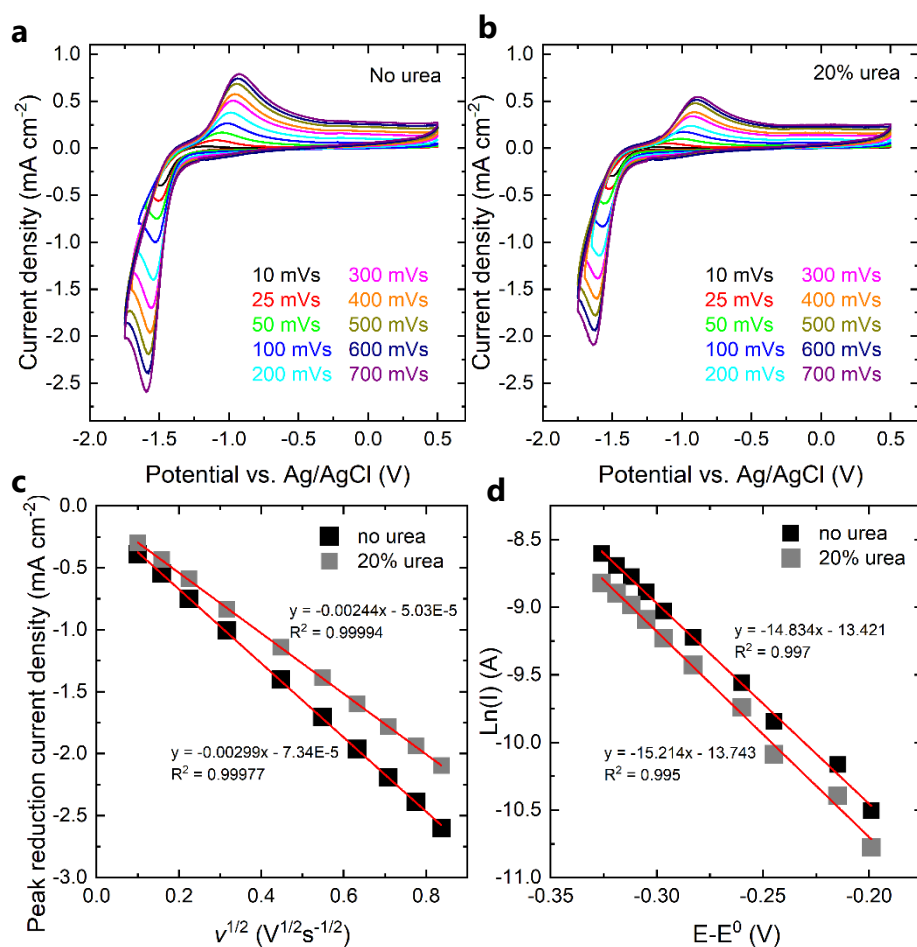


Fig. S10: Kinetic analysis of CrPDTA reduction with or without urea. **a**, Cyclic voltammograms of 5 mM KCrPDTA solutions in 0.1 M Borate buffer and 0.5 M KCl supporting electrolyte without or **b**, with 20% urea. Glassy carbon and Ag/AgCl electrodes were used as working or reference electrode, respectively. **c**, Peak reduction current versus the square root of the scan rate, with linear fit. **d**, Natural log of the peak reduction current versus the difference in potential between the voltage at the peak reduction current and the E^0 (-1.31 V vs. Ag/AgCl) of the reduction.

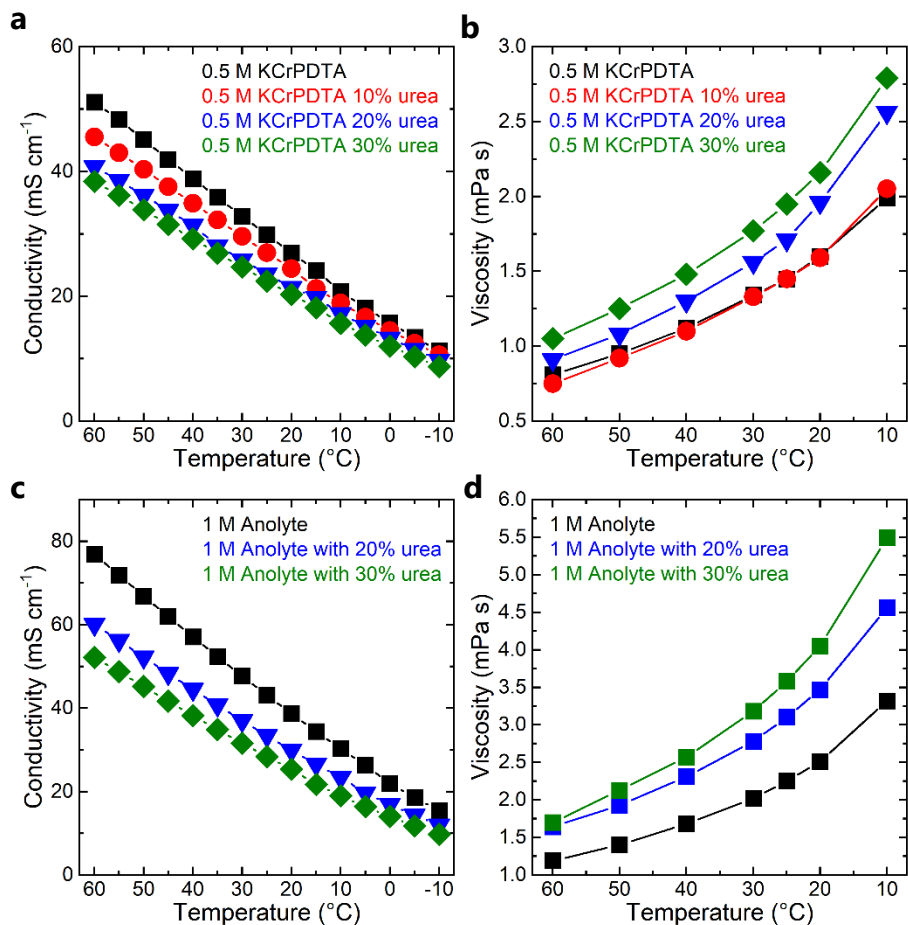


Fig. S11: **a**, Conductivity and **b**, viscosity of 0.5 M electrolytes with or without urea. **c**, Conductivity and **d**, viscosity of buffered 1 M KCrPDTA anolytes with or without urea.

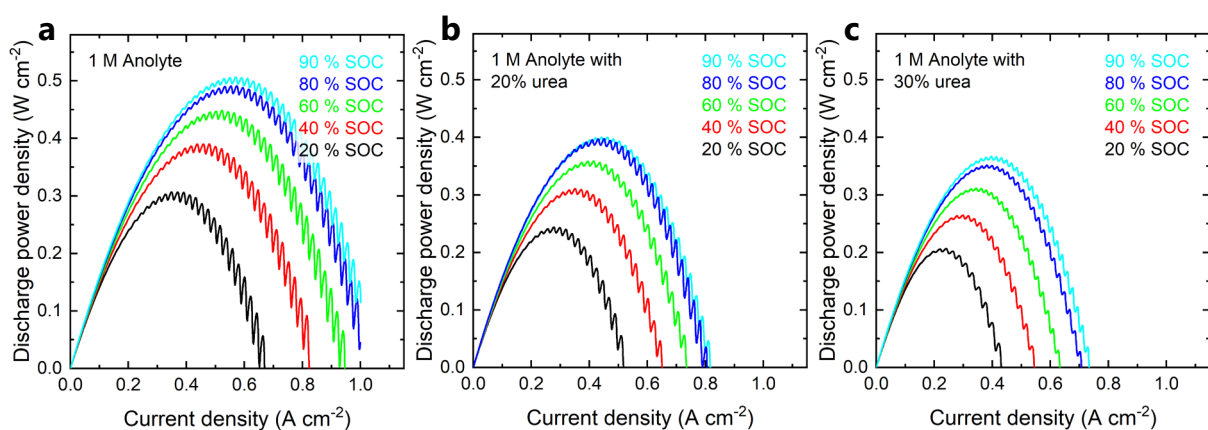


Fig. S12: Discharge power density versus current density at various states of charge using 1 M KCrPDTA anolytes containing **a**, no urea, **b**, 20% urea, or **c**, 30% urea. Oscillation of the current response is due to the pulsed electrolyte flow from the peristaltic pump.

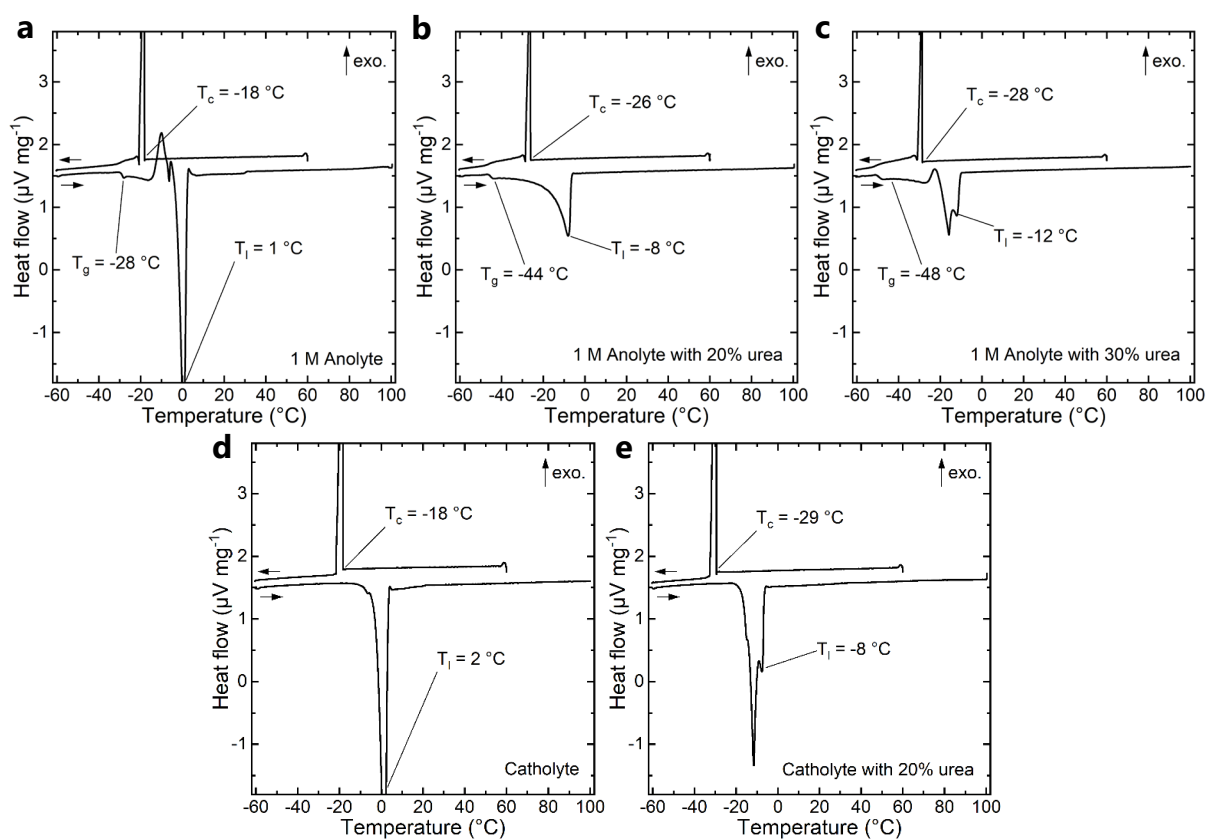


Fig. S13: **a**, Differential scanning calorimetry curves of 1 M KCrPDTA anolyte without urea and **b**, 20%, or **c**, 30% urea. **d**, 0.5 M $\text{K}_4\text{Fe}(\text{CN})_6 + 0.1\text{M K}_3\text{Fe}(\text{CN})_6$ catholyte without, and **e**, with 20% urea. Scans were recorded from 60 to -60°C and back to 100°C at a scan rate of $1^{\circ}\text{C min}^{-1}$. All samples were mixed with a small amount of meso-carbon microbeads to provoke crystallization.

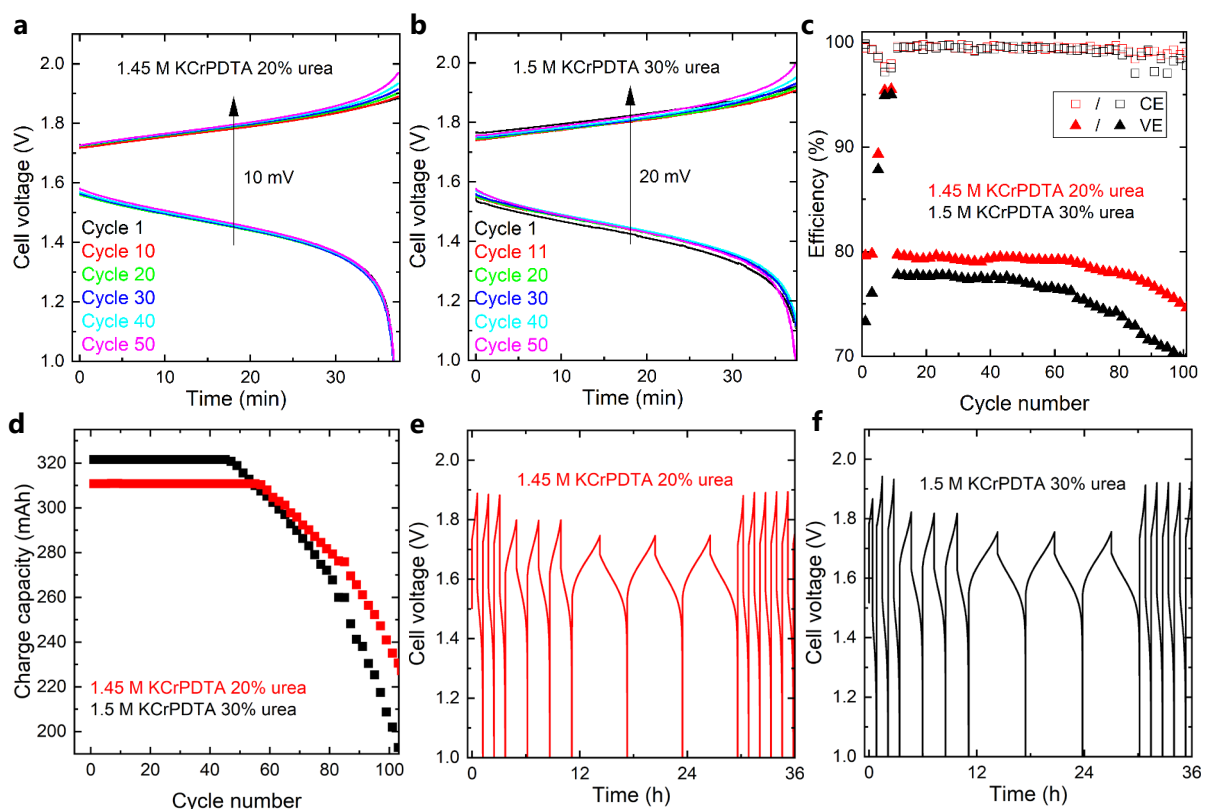


Fig. S14: Voltage profiles of the cells shown in Figure 5a using **a,e**, a 1.45 M KCrPDTA 20% urea anolyte, and **b,f**, a 1.5 M KCrPDTA 30% urea anolyte. **c**, Coulombic efficiency (CE) and voltage efficiency (VE) and **d**, charge capacity of the cells shown in Figure 5a for the full 100 cycles.

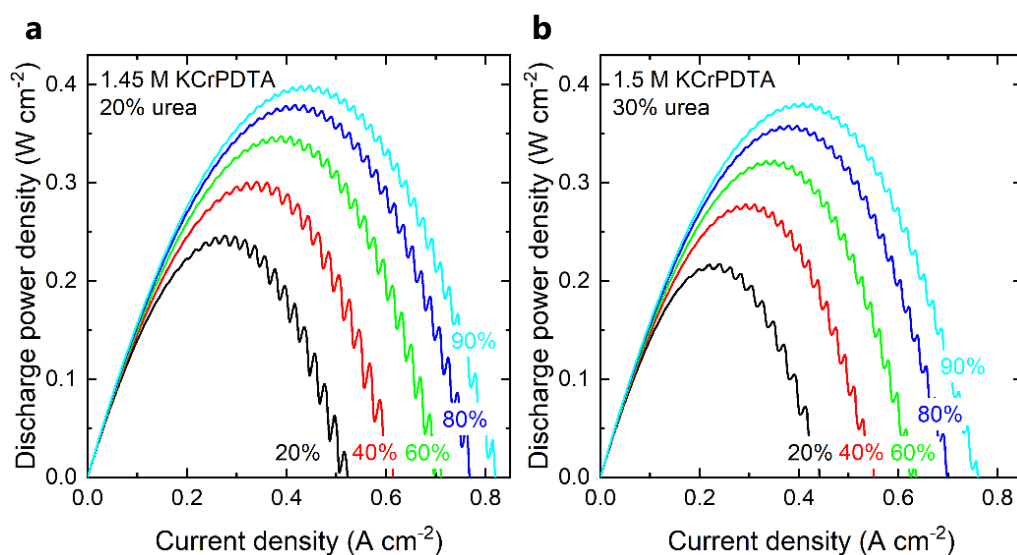


Fig. S15: Discharge power density versus current density at various states of charge using **a**, 1.45 M KCrPDTA 20% urea or **b**, 1.5 M 30% urea anolytes as for the cells shown in Figure 5. Oscillation of the current response is due to the pulsed electrolyte flow from the peristaltic pump.

Table S1: UV-Vis absorbance data for the examined complexes.

Compound	Wavelength [nm]	Molar absorptivity [$M^{-1} L^{-1}$]
$Fe(CN)_6^{4-}$	320	315 [2]
	420	1130 [2]
$CrPDTA^{1-}$	382	83 [3]
	506	116 [3]
$CrEDTA^{1-}$	390	113 [3]
	540	204 [3]
$CrCyDTA^{1-}$	390	97 [3,4]
	542	204 [3,4]

References

- [1] Y.M. Jung, B. Czarnik-Matusewicz, S. Bin Kim, Characterization of concentration-dependent infrared spectral variations of urea aqueous solutions by principal component analysis and two-dimensional correlation spectroscopy, *J. Phys. Chem. B.* 108 (2004) 13008–13014.
<https://doi.org/https://doi.org/10.1021/jp049150c>.
- [2] M.H. Panckhurst, K.G. Woolmington, A spectrophotometric study of ionic association in aqueous solutions, *Proc. R. Soc. London. Ser. A. Math. Phys. Sci.* 244 (1958) 124–139.
- [3] M. Hecht, F.A. Schultz, B. Speiser, Ligand structural effects on the electrochemistry of chromium (III) amino carboxylate complexes, *Inorg. Chem.* 35 (1996) 5555–5563.
<https://doi.org/https://doi.org/10.1021/ic960152o>.
- [4] N. Tanaka, K. Kanno, T. Tomita, A. Yamada, Synthesis and properties of sodium trans-1,2-cyclohexane-diaminetetraacetatochromate (III), *Inorg. Nucl. Chem. Lett.* 7 (1971) 953–956.
[https://doi.org/https://doi.org/10.1016/0020-1650\(71\)80008-9](https://doi.org/https://doi.org/10.1016/0020-1650(71)80008-9).